

Article

# Morphodynamic Study of a 2018 Mass-Stranding Event at Punta Umbria Beach (Spain): Effect of Atlantic Storm Emma on Benthic Marine Organisms

Juan García-de-Lomas <sup>1,\*</sup>, Andrés Payo <sup>2</sup>, Jose A. Cuesta <sup>3</sup> and Diego Macías <sup>4</sup><sup>1</sup> I+D Group on Structure and Dynamics of Aquatic Ecosystems, University of Cádiz, 11510 Cádiz, Spain<sup>2</sup> British Geological Survey, Marine Geosciences. Nicker Hill, Keyworth, Nottingham NG12 5GG, UK; agarcia@bgs.ac.uk<sup>3</sup> Instituto de Ciencias Marinas de Andalucía (CSIC), Avda. República Saharaui, 2, Puerto Real, 11510 Cadiz, Spain; jose.cuesta@icman.csic.es<sup>4</sup> European Commission, Joint Research Centre, Directorate D- Sustainable Resources, Via E. Fermi, 21027 Ispra, Varese, Italy; diego.macias-moy@ec.europa.eu

\* Correspondence: juan.garciadelomas@uca.es; Tel.: +34-678-623-308

Received: 31 May 2019; Accepted: 25 September 2019; Published: 30 September 2019



**Abstract:** Very few mass stranding events of invertebrates have been reported. In this paper, we report a mass stranding of multiple benthic organisms occurred at Punta Umbría beach (S Spain) after the passage of storm Emma (28 February to 5 March 2018). The most abundant organisms were identified, and exceptional meteorological and oceanographic events were analyzed, as a basis to understand the causes of stranding. The morphodynamic changes affecting the beach profile during the storm were inferred using a cross shore depth-integrated and time averaged numerical model (CSHORE). Among the stranded species, decapods (*Upogebia* spp., *Atelecyclus undecimdentatus*), sipunculids (*Sipunculus nudus*), starfish (*Astropecten* sp.), and sessile tunicates were dominant. Storm Emma involved extreme significant wave heights of up to 7.27 m, low pressures, strong SW winds, precipitations and spring tides that modified the seabed elevation to depth as deep as −10 m. Simulations suggest that benthic organisms living at a water depth between −10 to −0.3 m were buried under a layer of sediment of up to ca. 10 cm deposited during the storm. This burial preceded the transport of intertidal and subtidal benthic organisms to the dry beach, causing their stranding. Impacts on the quality of habitat, biodiversity and the productivity of coastal ecosystems are discussed.

**Keywords:** mortality; starfish; invertebrate; *Upogebia*; storm; breakwater

## 1. Introduction

There is a vast literature on the stranding of marine vertebrate species (particularly cetaceans); however, very few stranding and mass mortality of invertebrates have been reported. The most frequent biotic causes of mass-mortality events include toxicity, due to toxic algal blooms [1,2], the appearance of diseases [3,4], or mortality following spawning events. Among the abiotic causes, the most frequent are storms, currents or strong waves, changes in temperature and salinity, hypoxia, emersion during low tide or oil spills [5]. In the particular case of storms, benthic invertebrate mortality can occur either because they are covered by sediment or because they are dragged to the dry beach [6]. In any case, mass mortalities or strandings usually affect one single species [5,7–10], and there are hardly any reported cases that affect multiple taxonomic groups.

Except for mortalities following spawning [11], which can be considered a natural and periodic event, all other cases of strandings are related to extreme and unexpected events, which make them difficult to forecast or in depth analyze. This eventuality limits the amount of information that can

be obtained and consequently, a large part of the strandings that occurs does not go beyond mere news in the local press, with little information provided. For example, ‘millions’ of *Colochirus ocnoides* and a large number of young *Caudina coriacea* (Echinodermata, Holothuroidea) were found in the New Zealand beach of Christchurch in the winter of 1897 [12]. ‘Hundreds’ of starfish (*Asterias rubens*) were observed after a severe storm in 1902 at the beach of Yarmouth (Nova Scotia, Canada) [13]. Additionally, ‘hundreds’ of holothuroidea *Myriotrochus rinkii* (Echinodermata, Holothuroidea) were observed at Point Barrow, Alaska, after severe storms [14]. The mass mortality of *Echinocardium cordatum* in the north of the Gulf of Aqaba in 1972 was documented [15]; and the mass mortality of *Cassidulus caribbearum* on the seafloor in the Virgin Islands was caused by strong storms [16]. More recently, a mass stranding of starfish (*Asterias rubens*) were reported in the Isle of Man [9], and the south coast of England [10] coinciding with major spring tides in conjunction with strong winds and large swell.

This lack of solid scientific assessments contrasts with potential ecological and economic implications of such events. Mass mortality can suppose a reduction of the natural populations, altering the composition and functioning of the community and the ecosystem benefits to human beings. Depending on their magnitude, mass mortalities can be considered disasters, or even catastrophes. ‘Disasters’ occur with such frequency that they are likely to occur within the life cycles of successive generations, whereas, ‘catastrophes’ occur so rarely that they are unlikely to constitute a selective force [17]. This distinction is important when evaluating the consequence of mortalities. Likewise, the analysis of the possible causes may help to predict future mass mortalities and their consequences. Considering that climate change models suggest an increase in the frequency of extreme weather events [18], the analysis of strandings can shed light on their consequences on biodiversity, ecological processes and the maintenance of ecosystem services.

This paper documents the mass stranding of marine invertebrates that occurred on the beach of Punta Umbría, from March 4 to 8, 2018, coinciding with an Atlantic Ocean storm named Emma (February 28 to March 5, 2018). Similar previous data are not reported in existing literature, and thus, this paper serves as a baseline for this type of exceptional events, useful to compare the consequences of similar future happenings and evaluate if the same species are affected and in the same proportion. We identified the stranded organisms and their distribution in the beach following storm Emma. We also gathered the meteorological and oceanographic (met-ocean) conditions during the storm event and simulated the profile elevation change before, during and after storm Emma using the CSHORE numerical model [19]. Then we present the met-ocean more salient characteristics and the model-based morphodynamics of stranding. Our results provide some insights regarding the exceptional causes and ecological consequences of the stranding.

## 2. Materials and Methods

### 2.1. Study area

The El Portil-Punta Umbría area (Huelva), along the South-Western coast of the Atlantic Ocean in Spain has an extension of 10.5 km, and is located between the mouth of the Piedras river, at its western end, coinciding with the tip of the Rompido spit, and the Punta Umbría jetty (constructed between 1984 and 1986), at its eastern end, which protects the outlet of the Ciate channel, former arm of the mouths of the Tinto and Odiel rivers (Figure 1). It is a sandy spit and barrier island resulting from the effects of the coastal hydrodynamic regime that has been modelling this coast since the last postglacial transgression. In more recent times, the construction of two dams between 1981–1986 drastically modified the coastal morphology and sedimentary dynamics in this area [20].



**Figure 1.** Punta Umbría Beach, where the mass stranding of marine organisms took place between the 4th and 8th of March, 2018. The distribution of the maximum accumulations of organisms is shown in the enlarged image (2.4 ha).

The coast is affected by a meso-tidal regime with an average tide range of 2.2 m (maximum range in spring tides = 3.7 m, and in neap tides = 0.7 m). The average significant wave height ( $H_s$ ) in the study area is 0.7 m and an average wavelength of ca. 40 m acts on the open systems of the coast. The dominant waves come from the southwest (SW), and the beach is orientated ca. 118 deg measured clockwise to the North, which gives rise to a coastal drift that transports sediment from west to east and that is responsible for the construction of the beaches and the sandy formations located in front of the fluvial estuaries [21]. The climate in the Mediterranean consists of hot and dry summers, and mild and humid winters. The average temperature and precipitation measured at the Huelva weather station (located 11 km from the area of study) for the period 1984–2010 is 18.2°C and 525 mm, respectively [22], with a marked intra- and inter-annual variability of precipitation. Consequently, the rivers present a highly irregular flow, with a significant seasonal and inter-annual variation. The area of study can be considered as a well-preserved coastal area with a high natural value, surrounded by several protected maritime areas included in the European Natura 2000 Network, such as the ‘Enebrales de Punta Umbría’ (SCI 187 ha), ‘Piedras River Marshes and Rompido Spit’ (SCI-SPA, 2,409 ha) and the ‘Odiel Marshes’ (SCI-SPA, 6,618 ha) and has meadows of *Zostera noltii* and *Cymodocea nodosa* (the latter in regression) in the mouth of the Piedras river [23].

## 2.2. Identification of the stranded organisms

The location of the organisms stranded on the stretch El Portil-Punta Umbría (10.5 km), between the mouths of the Piedras River and the Ciate Channel was first analyzed. The stranded organisms were identified on March 8th. Specialized keys were used for the decapod crustaceans (Gebiidea) [24], and for the rest of decapods [25]. The guide [26] was used for molluscs. It was not possible to reliably quantify the abundance of stranded organisms due mainly to three reasons: (i) Four days passed after the first news that a mass stranding of starfish was reported. At that time, a portion of the stranded organisms (e.g., starfish) had been washed away by the tides, as some locals reported; (ii) numerous organisms were selectively collected by local shellfish catchers (e.g., starfish, sipunculids, molluscs, and polychaetes) (Figure 2d), either as bait for sport fishing or for decorative purposes; and (iii) predation

by seabirds of the stranded animals (Figure 2e). Information on species abundance and biomass could have enriched the discussion and strengthen the conclusions reached in this paper. Despite these limitations, however, we provide a semiquantitative category of relative abundance for each organism (rare, occasional, frequent, abundant, and dominant) based on in situ observations. Also, the most abundant organisms were recorded, and, in the case of *Upogebia deltaura* and *U. pusilla* (Crustacea, Decapoda, hereinafter *Upogebia* spp.), as clearly the most abundant group (Figure 2c, Figure 3a,b), the measurement of abundance was made in  $n = 8$  quadrats of  $0.25 \text{ m}^2$  as a proxy to the order of magnitude of the stranding.



**Figure 2.** General view of the mass stranding at Punta Umbría beach, showing the stranding of marine organisms (a–e), nets and anthropogenic wastes (b). Collection of some stranded taxa by local fishers (d) and predation by waterbirds (e,f). Effects of storm Emma on beach erosion, close to the mouth of the Piedras river (g).

**Table 1.** Organisms stranded on the beach during the massive stranding occurred during March 4–8, 2018. The symbols indicate a semiquantitative category of relative abundance: Rare (r), occasional (o), frequent (f), abundant (a), and dominant (d).

Phylum, Class	Taxa
Mollusca, Gastropoda	<sup>o</sup> <i>Bolinus brandaris</i> , <sup>o</sup> <i>Euspira catena</i> , <sup>o</sup> <i>Nassarius incrassatus</i> , <sup>f</sup> <i>Cymbium olla</i> *.
Mollusca, Bivalvia	<sup>f</sup> <i>Solen marginatus</i> , <sup>f</sup> <i>Pharus legumen</i> , <sup>o</sup> <i>Acanthocardia tuberculata</i> , <sup>o</sup> <i>Anomia ephippium</i> , <sup>o</sup> <i>Diplodonta rotundata</i> , <sup>o</sup> <i>Loripes lucinalis</i> , <sup>o</sup> <i>Dosinia exoleta</i> , <sup>o</sup> <i>Lutraria lutraria</i> , <sup>f</sup> <i>Mactra stultorum</i> .
Crustacea, Malacostraca	<sup>a</sup> <i>Ateacyclus undecimdentatus</i> , <sup>f</sup> <i>Dardanus arrosor</i> , <sup>d</sup> <i>Upogebia deltaura</i> , <sup>d</sup> <i>Upogebia pusilla</i> , <sup>r</sup> <i>Goneplax rhomboides</i>
Sipuncula, Sipunculidae	<sup>a</sup> <i>Sipunculus nudus</i>
Echinodermata, Asteroidea	<sup>a</sup> <i>Astropecten</i> sp.
Echinodermata, Ophiuroidea	<sup>r</sup> <i>Ophiura</i> sp.
Echinodermata, Echinoidea	<sup>o</sup> <i>Echinocardium cordatum</i>
Echinodermata, Holothuroidea	<sup>o</sup> <i>Holothuria</i> sp.
Annelida, Polychaeta	<sup>o</sup> <i>Hediste diversicolor</i>
Chordata (Tunicata), Ascidiacea	<sup>a</sup> <i>Phallusia mammillata</i>
Chordata, Actinopterygii	<sup>r</sup> <i>Solea</i> sp.
Chordata, Chondrichthyes	<sup>r</sup> <i>Scyliorhinus canicula</i>

\* Only empty shells were found.

### 2.3. Meteorological and oceanographic conditions

The meteorological conditions during the storm event, including air temperature (°C), precipitation (mm), wind speed (km/h) and wind direction (reported by the direction from which it originates), were recorded and provided by the City of Huelva weather station (37°16'42" N; 6°54'42" W), located less than 12 km from the site of stranding. The oceanographic data were obtained from the 'Portus' database from 'Puertos del Estado' official website (<http://www.puertos.es/en-us/oceanografia/Pages/portus.aspx>). The data (with hourly time resolution) on significant wave height,  $H_s$ , wave peak period,  $T_p$ , and wave direction,  $\theta_N$ , were obtained from the directional wave buoy of the Gulf of Cadiz, anchored at a depth of 450 m (36°28'48" N; 6°57'36" W).

On the other hand, data on atmospheric pressure, sea level and port agitation (i.e., water level oscillations inside a port basin) were obtained from the Huelva 5 tide gauge (37°7'48" N; 6°49'48" W), located inside the Mazagón marina, 11 km from the site of stranding. As the tide gauge is sheltered from wind waves (i.e., wave periods between 1 and 30 s), the sea level data recorded by the tide gauge are not affected by the wind swell, and their oscillations are mainly due to a combination of astronomical and meteorological tides. From 'Puertos del Estado' website, the hourly time series of the different oceanographic variables were downloaded from 12:00 21/02/2018 to 23:00 11/03/2018.

### 2.4. Model-based morphodynamics of stranding

The morphodynamic changes during the storm were simulated using the CSHORE numerical model [19]. CSHORE is a profile morphodynamic model (e.g., it assumes longitudinal beach uniformity) that solves the time and depth-averaged continuity and conservation of energy equations to estimate the alongshore and across shore sediment transport, the associated bathymetric changes, as well as other engineering variables of interest, such as overwash heights. The input parameters of the model are the beach profile elevation, average grain size ( $d_{50}$ ) of the sediment, boundary conditions at the seaward end of the profile (root mean square wave height,  $H_{rms}$ , peak period,  $T_p$ , and direction,  $\theta$ ,

and the surge and sea level, due to the astronomical and meteorological tides) (see Supplementary Materials). The wave direction  $\theta$  in CSHORE is the incident angle relative to the shore normal at the study site (convention is positive counterclockwise).

Due to the lack of hydrodynamic and sediment transport observations during the storm event, the default values recommended by [19] were used (Appendix A). The hourly wave time series from Puertos del Estado of  $H_s$ ,  $T_p$ ,  $\theta_N$  and Sea Level was used as boundary conditions at the seaward end ( $x = 0$ ) of the bottom profile. We have used the relationship  $H_s = 1.42 \times H_{rms}$  [27], to convert the recorded  $H_s$  to  $H_{rms}$ . The wave direction relative to the North,  $\theta_N$ , was converted to wave direction relative to the beach normal at the study site as  $\theta = 208 \text{ deg} - \theta_N$ , where 208 deg is the direction of the shore normal measured clockwise relative to the North (i.e., shore is orientated 118 deg clockwise to the North) at the study site. Waves coming from wave angles  $\theta_N$  larger than 208 deg will result in  $\theta < 0$  (i.e., longshore sediment transport is from El Portil towards Punta Umbria) and  $\theta_N$  smaller than 208 deg will result in  $\theta > 0$  (i.e., longshore sediment transport is from Punta Umbria towards El Portil).

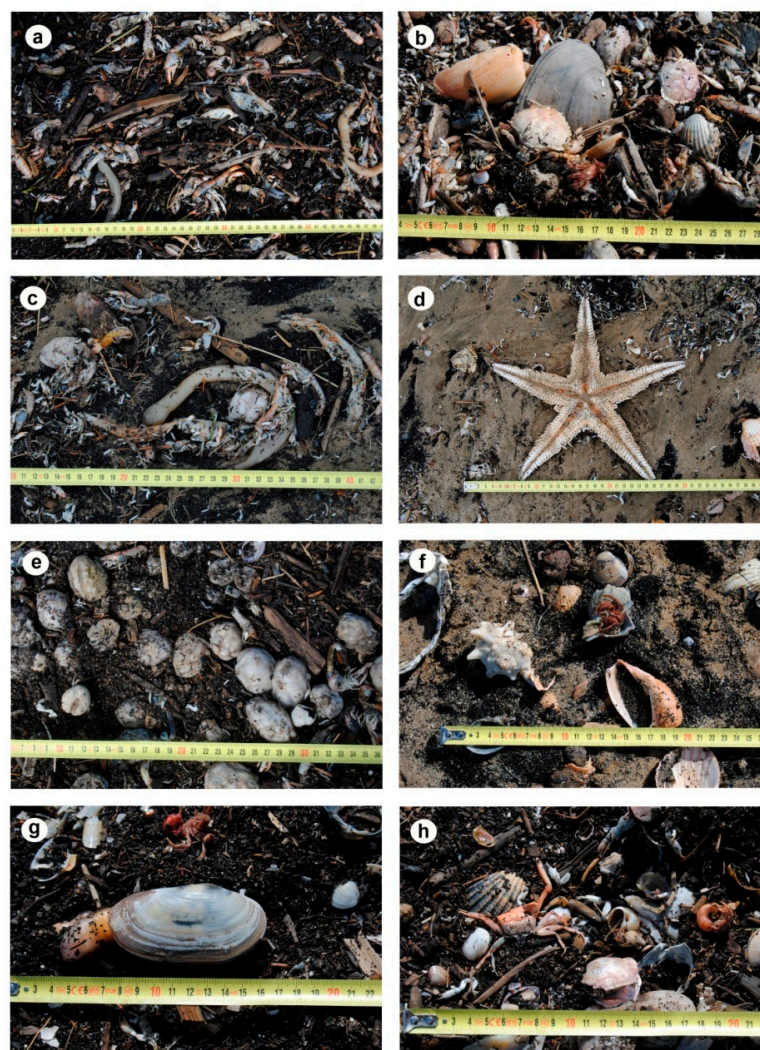


**Figure 3.** Main organisms observed in the mass stranding occurred at Punta Umbría beach during storm Emma (see Table 1 for details). (a) A mix of benthic invertebrates, showing the dominance of *Upogebia* spp.; (b) crabs *Atelecyclus undecimdentatus* and *Dardanus arrosor* (out of the typical protective shell); (c) *Upogebia* spp., *Sipunculus nudus* and some tunicates; (d) starfish of the genus *Astropecten*; (e) the tunicate *Phallusia mamillata*; (f) shells of *Cybium olla* and *Bolinus brandaris*; (g) the bivalve *Lutraria lutraria*; (h) the crab *Goneplax rhomboides*, shells of *Euspira* sp. (Gastropoda) and *Anomia ephippium* (Bivalvia).

The input beach profile was obtained by combining the topographic data of the beach presented by [28], and those taken from the nautical map of the area at a scale of 1:50000 along a transect perpendicular to the beach. Figure 4 shows the approximate location of the transect along which the topography and bathymetry have been extracted. The bottom elevation along the perpendicular transect to the beach, from the hydrographic zero up to 100 m water depth were extracted from the nautical map of the area at the intersection of the bathymetry contour lines and the transect.

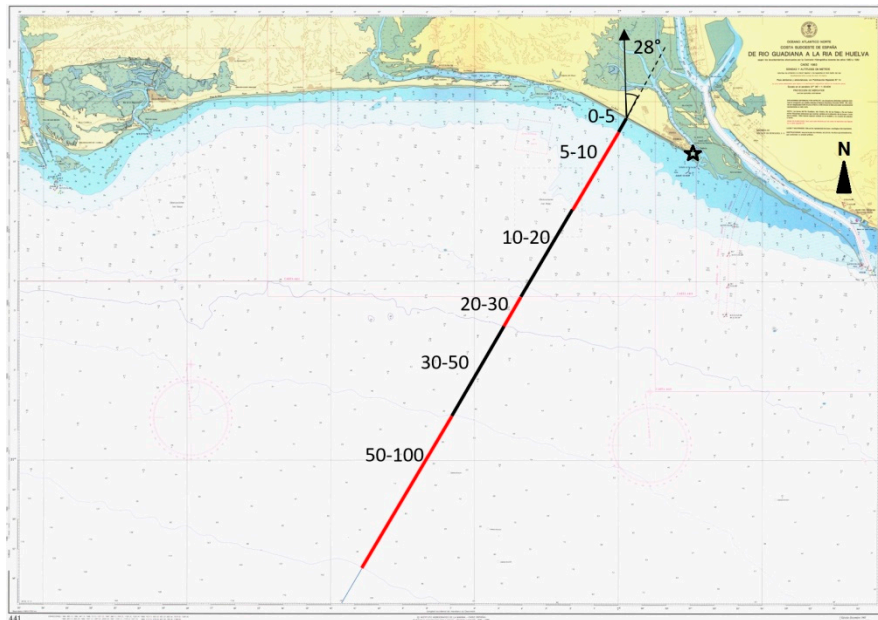


**Figure 4.** Transect perpendicular to Punta Umbría beach along which the topo-bathymetric profile representative of the study area has been extracted (the star indicates the location of the stranding). The red and black segments indicate the segments between the different bathymetric lines (e.g., 0–5 is the segment between the bathymetric lines 0 and 5 m).

Reference [28] showed how beach profiles throughout the study area differ according to the most recent history of oceanographic conditions, thus, differentiating between more reflective and temporary or more dissipative good weather profiles. For this study, we have selected the winter profile corresponding to transect number 9 located in the vicinity of the stranding area [28]. This transect was selected as it was closest to the stranding and was published on an open access peer-reviewed journal. The winter profile was chosen for the observation in the storm series of waves, due to the existence of storms during the month prior to storm Emma. The bottom elevation data from the depth of ca.  $-1$  m to ca.  $+8$  m were extracted from the winter Huelva area profile number 9, shown in Figure 4 in [28]. The elevations provided by [28], and the nautical charts are referenced to the hydrographic zero and were merged to produce a topo-bathymetric profile from  $-100$  m water depth to ca.  $+8$  m elevation. It was assumed that the average grain size was  $d_{50} = 0.42$  mm, according to observations made by [28] for this profile during winter.

### 3. Results

#### 3.1. Distribution of the stranded animals and major taxa

In the prospected section, the stranded animals were concentrated exclusively in the vicinity of the Punta Umbría breakwater, in a band of approx. 1.3 km (Figure 1). Stranded animals were added in bands of variable width along the sandy intertidal area, apparently segregated by size: Smaller soft-body organisms, such as decapods and polychaetes were more abundant near the shore, while larger organisms, such as *Cybbium olla* shells and tunicates (Figure 3e), as well as numerous

anthropogenic wastes (nets, traps, pots, etc.), were concentrated near the high tide line (Figure 2b). Most of the stranded animals appeared on dark macrodetritus (cohesionless, organic particles >0.5 mm) (Figures 2 and 3) whose observation at the dissecting microscope revealed that it consisted mainly of plant remains.

Most of the taxa observed (23 out of 26) were benthic invertebrates, with the exception of tunicates and isolated specimens of fish, such as *Solea* sp. and *Scyliorhinus canicula* (Table 1). The most abundant taxa were mud shrimp (*Upogebia deltaura* and *U. pusilla*) (Figures 2c and 3a,b), sipunculid (*Sipunculus nudus*) (Figure 3a,c), the crab *Atelecyclus undecimdentatus* (Figure 3b) and the hermit crab *Dardanus arrosor* (Figure 3f,g). Sand starfish of the genus *Astropecten* (Echinodermata) (Figure 3d), bivalve molluscs (e.g., *Pharus legumen*, *Lutraria lutraria*, *Loripes lucinalis*, *Acanthocardia tuberculata*, *Solen marginatus*) (Figure 3g), gastropods (e.g., *Bolinus brandaris*, *Euspira* sp.) (Figure 3f,h) and tunicates (mainly *Phallusia mammillata*) (Figure 3e) were also abundant (Table 1). In the specific case of *Upogebia* spp., an average of 248 indiv/m<sup>2</sup> (n = 8) was counted. Taking into account only the area where the greatest accumulations of stranded organisms were found (about 2.4 ha) (Figure 1) and omitting any predation by seabirds as the animals reached the shore (Figure 2f), the stranding may have affected approximately 5.9 million *Upogebia* spp. individuals.

### 3.2. Met-ocean conditions

Between February 28 and March 5 of 2018, several exceptional meteorological and oceanographic conditions were registered:

- Elevated heights of significant swell ( $H_s$ ), especially on March 1 (between 4.92–7.27 m) (Figure 6a). More specifically, at 3:00 p.m. (2:00 p.m. GMT) a value of  $H_s = 7.27$  was reached, which is the highest known value in the period of 1996–2018, surpassing its previous record of 6.6 m recorded in April of 2003.
- Swell of an almost normal incidence to the coast, with average angles of 30 degrees and maximum and minimum values of 42 and 18 degrees, respectively. The beach line in the stranding area has an orientation of about 28 degrees to the north (Figure 6c).
- Water levels (taking into account the sum of the astronomical and meteorological components) of up to 4.12 m on March 1 to 3 (Figure 6d), respectively. Curiously, the moment of the greatest wave height (from 7.27 m at 3:00 p.m. on March 1) coincided with the high tide. This sea height was the highest recorded in the entire year of 2018.
- Low pressures between February 28 and March 2, under 1000 mb, with a minimum of 987 mb on March 1 (Figure 5a).
- Strong winds from the SW-W from March 1 to March 6 (Figure 5b), including a tornado on March 4, 2018, between 5:40 and 7:00 p.m., approximately (<https://sinobas.aemet.es/>);
- Torrential rains between February 28 and March 2 (total 113 mm) (Figure 5c).

These phenomena coincided with the passage of storm Emma. Warnings of waves of up to seven meters were issued by the Spanish Meteorological Agency (AEMET) on February 28, 2018.

The observed peak wave periods (Figure 6b) and port agitation data suggest that most of the wave energy was within the expected wave period of wind swell between 5 and 12 s during storm Emma. The wave buoy is limited, by design of the measurement system, to maximum wave periods of 30 s, so that the absence of wave peak periods in these frequencies does not always imply that there was no wave energy of longer periods. The agitation data from the Mazagón port, on the other hand, was measured continuously at frequencies of 2 Hz, making it possible to detect long-period swells (i.e., >30 s). However, the agitation data during storm Emma inside the harbor did not exceed 0.51 m and 7 s periods suggesting the absence of long waves.

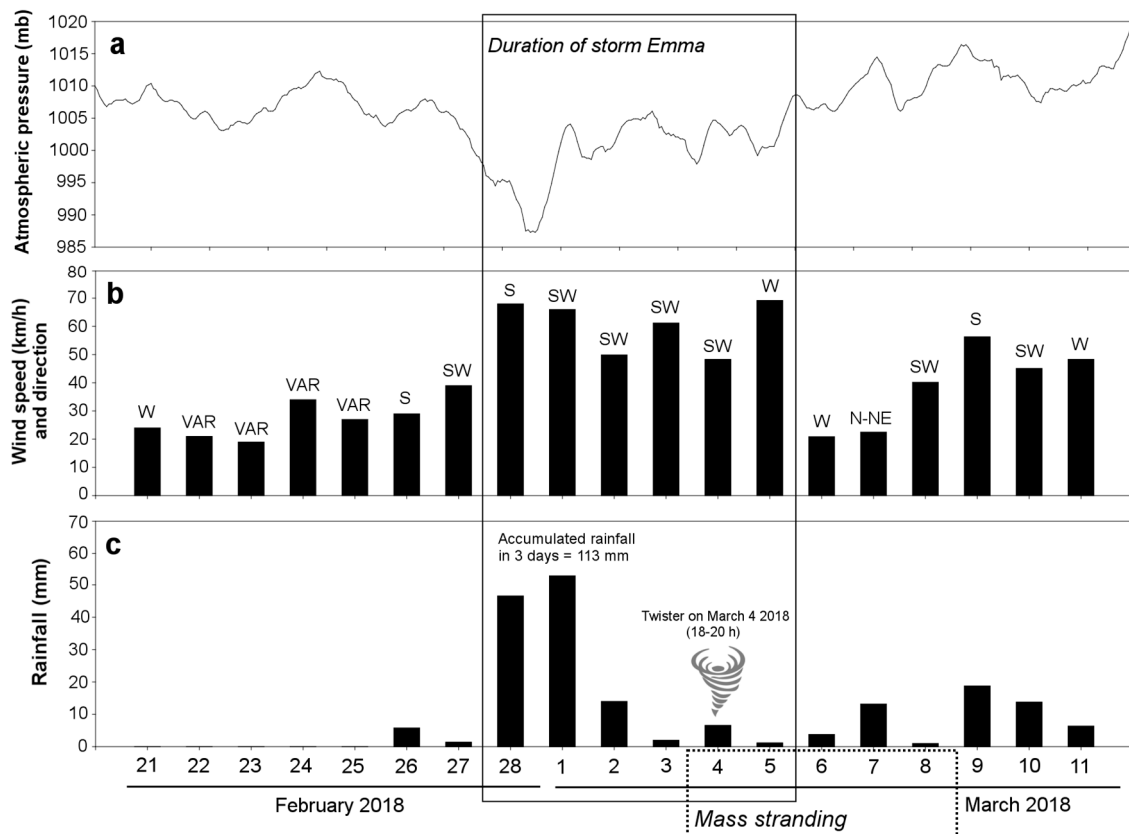


**Figure 5.** Climatic variables before and after the mass stranding of marine benthic animals: (a) Atmospheric pressure; (b) wind speed and wind direction; (c) daily rainfall.

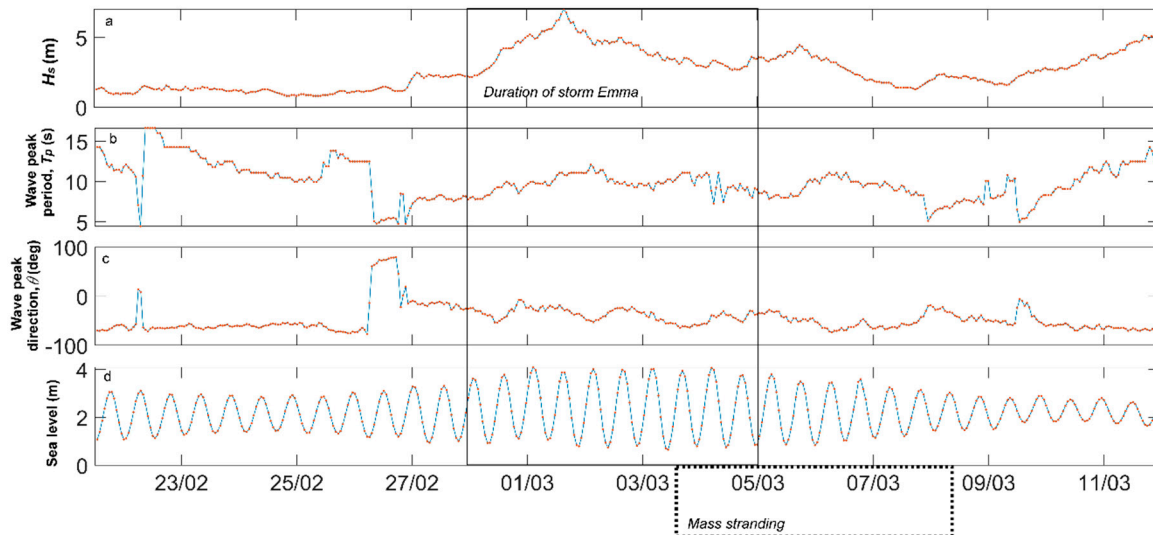
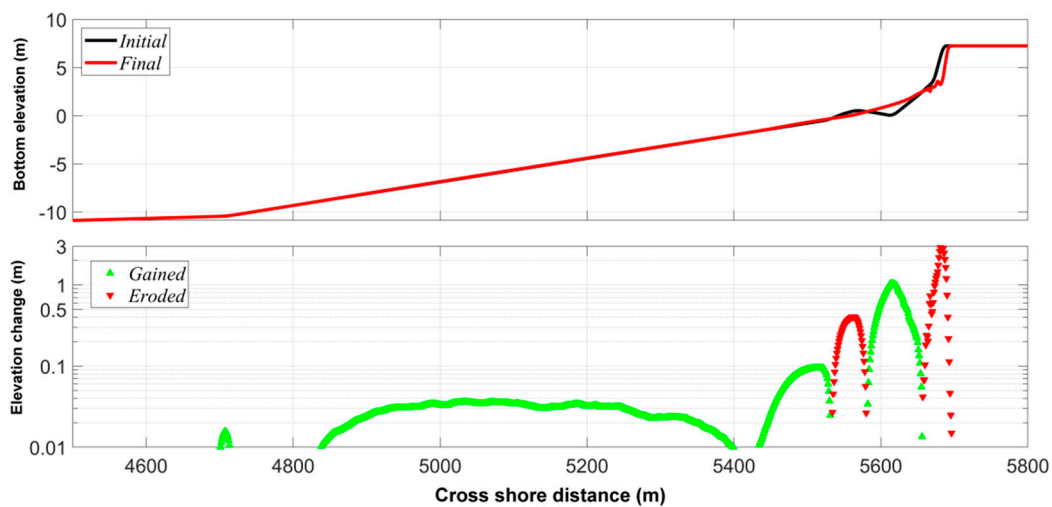


**Figure 6.** Oceanographic variables before and after the mass stranding of marine benthic animals: (a) Significant wave height,  $H_s$ ; (b) wave peak period,  $T_p$ ; (c) incident wave direction relative to shore normal,  $\theta$ ; and (d) water level.

Figure 7 shows the profile at the beginning and the end of the passage of the storm. The results of the simulation show how a vertical scarp occurred on the dry beach and how the typical winter profile with a submerged bar was transformed into a flat beach where the eroded material of the dune and the

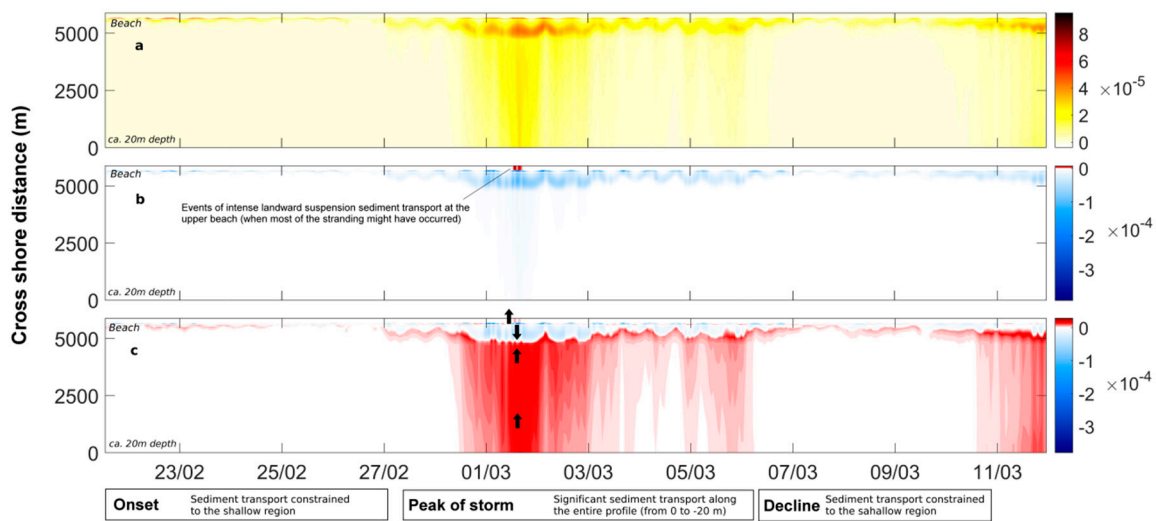
subtidal zone was deposited in the intertidal zone. Throughout the transect, alternate areas of gain and loss of bottom elevation were observed:

- In the area between the  $-20$  m to  $-10$  m depths with respect to the hydrographic 0, erosion was always less than  $-1$  mm;
- Between the depths of ca.  $-10$  to  $-0.3$  m there was an area of elevation gain with maximum values of up to  $+9.4$  cm;
- Between the depths of  $-0.3$  to  $+7$  m, there were alternate areas of gain and loss of elevation associated with the transition from a bar profile to a profile of a uniform slope to the escarpment of the dune where the highest elevation losses of  $-2.5$  m were observed;



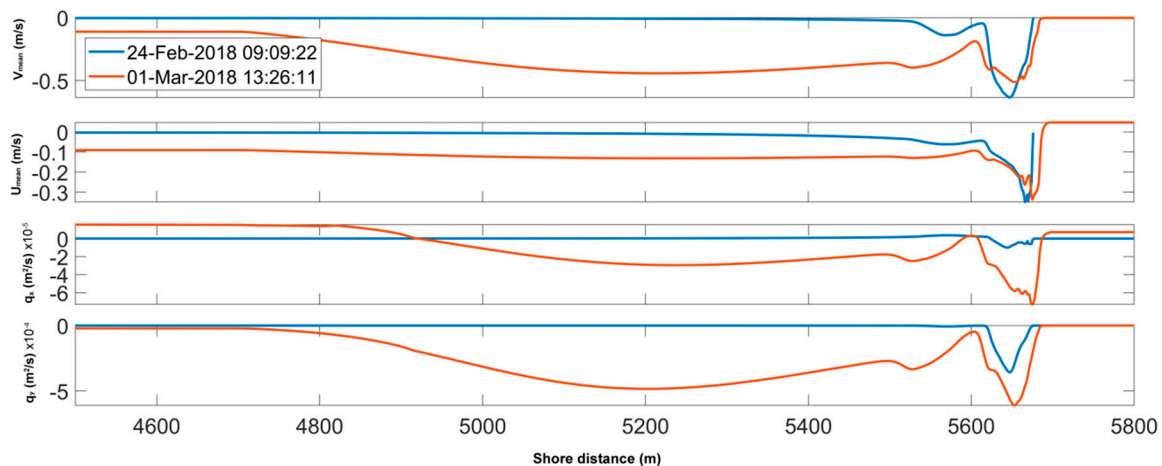
**Figure 7.** (a) Initial and final topo-bathymetric profiles and (b) elevation change according to the morphodynamic model.

Figure 8 shows the depth-integrated and time averaged bedload, suspended and total (i.e., combined bedload and suspended) cross shore sediment transport rates according to the morphodynamic simulation. During non-storm conditions, before and after storm Emma, most of the cross shore sediment transport is limited to the shallow zone region of the profile (zone of depths lower than ca.  $-7.0$  m), while during storms conditions the cross shore sediment transport is significant ( $>0$   $\text{m}^2/\text{s}$ ) along the entire simulated beach profile (from the depth of  $-20$  m up to the dry beach). By definition in CSHORE, the direction of the simulated cross shore bedload sediment transport is always from sea to land (i.e., positive values), while the direction of the sediment transport in suspension and total sediment transport varies along the profile, with regions where the direction is seaward (i.e., negative values) and regions where the direction is landward. This change of direction of the suspended and total sediment transport is more evident during storm conditions when the total transport is landwards for depths between ca.  $-20$  m to  $-10$  m (i.e., dominated by the onshore bedload sediment transport) and seawards for depths between ca.  $-10$  m to the low swash area (i.e., area that is always submerged).



**Figure 8.** Transport of sediments according to the model: (a) Bed load, (b) suspended load and (c) total load (combined bed and suspended load). Arrows on panel (c) show the net direction of sediment transport during the peak of the storm (arrows up indicate transport towards the beach, whereas, arrow down indicates transport towards the open sea).

Figure 9 shows a comparison of the cross shore variation of sediment transport and hydrodynamic conditions during non-storm conditions (24/02/18 and  $H_{rms} = 0.87$  m at  $x = 0$ ) and during the peak of the storm (01/03/18 and  $H_{rms} = 4.43$  m at  $x = 0$ ). As mentioned above, during storm conditions the entire profile (i.e., from depth -20 m to 0 m) is active, while during non-storm condition only the shallowest section of the profile is active. Interestingly, the maximum depth-integrated longshore current velocity,  $V_{mean}$ , is observed during non-storm conditions where  $V_{mean} = -0.62$  m/s (i.e., the negative sign indicate that transport was from El Portil towards Punta Umbría) which is larger than the maximum value  $V_{mean} = -0.48$  m/s during the storm condition. Simulated wave-induced alongshore current is very sensitive to, among others, the shape of the profile, which was not measured during the storm event—therefore, the simulated values have to be interpreted with caution. The maximum depth-integrated cross shore current velocity,  $U_{mean}$ , was similar under storm and non-storm conditions and ca.  $-0.3$  m/s (i.e., the negative value sign indicate that current direction was offshore). The maximum total cross shore sediment transport,  $q_x$ , was one order of magnitude larger during the storm conditions,  $q_x \sim 7 \times 10^{-5}$  m<sup>2</sup>/s, than during non-storm conditions  $q_x \sim 7 \times 10^{-6}$  m<sup>2</sup>/s. The maximum total longshore sediment transport,  $q_y$ , during the storm conditions was ca. twofold ( $q_y = 6.0 \times 10^{-4}$  m<sup>2</sup>/s) the maximum value during non-storm conditions ( $q_y = 3.4 \times 10^{-4}$  m<sup>2</sup>/s). The sediment transport is the product of the sediment in motion and the cross shore or alongshore velocities. Since the differences on the maximum velocities under storm and non-storm conditions are of a similar order of magnitude, it suggests that the large differences on sediment transport between non-storm and storm conditions were mostly due to much higher volumes of sediment been in motion (i.e., either as bed load or suspended load) during the storm conditions.



**Figure 9.** Comparison of cross shore variation of sediment transport and hydrodynamic conditions during non-storm conditions (24/02/18) and during the peak of the storm (01/03/18).

## 4. Discussion

### 4.1. The Exceptionality of the stranding

The occurrence of a massive stranding during the first days of March 2018 coincided with the passage of storm Emma. Unlike other strandings in the SW of the Iberian Peninsula that affected specific taxonomic groups, such as *Physalia physalis* [29], algae [30] or molluscs [31], in this case, the variety of benthic organisms typical of intertidal and subtidal waters, mostly invertebrates, was of special interest. These animals are not usually seen as part of beach-cast remains on a regular basis and much less in a massive way, which suggests that the mortality documented in this paper was an exceptional event. On the other hand, many specimens were still alive, which would rule out any event of contamination, poisoning or diseases. Curiously, during the March 6th to 8th, the beaches of the Bay of Cadiz also experienced a mass stranding of *Physalia physalis* [32]. On these same dates and also coinciding with storm Emma, the stranding of ‘thousands’ of animals (including starfish, lobsters, clams, bryozoans, anemones and crabs among others) was reported on the shores of southern England (Ramsgate, Kent) [33,34]. Both localities (Ramsgate in England and Punta Umbría in Spain) have in common the presence of docks next to the place of stranding (in the first case, the docks are part of the port of Ramsgate). This suggests that docks could facilitate the concentration of organisms removed by the storm on specific sections of the dry beach.

Regarding the surface affected by the storm, both the biology of the organisms found and the presence of anthropogenic remains (some with obvious signs of wear and colonization of sessile organisms, probably lost or abandoned long ago, Figure 2b) suggest that the mortality affected both the intertidal, and part of the subtidal zones. For example, the decapods *Upogebia* spp. are typical of intertidal and subtidal or estuarine zones up to 45 m deep [35,36]. *Sipunculus nudus* inhabits the sandy intertidal area, inside non-permanent galleries 15–35 cm deep [37]. The sand urchin *Echinocardium cordatum* populates sandy bottoms up to 200 m deep and can be buried up to 20 cm in the substrate [38]. The bivalve *Pharus legumen* inhabits depth range of 5–25 m [39], whereas, *Lutraria lutraria* inhabits muddy sands at very low spring tides and offshore to a depth of 90 m [40]. Likewise, *Ophiura ophiura* can live from the low-water line up to 800 m deep. Therefore, the stranding of this varied array of benthic organisms highlights the power of severe storms to mobilize sediments and organisms to considerable depths and affect populations of organisms located some distance from the shore [41].

#### 4.2. Causes of stranding

The intense winds from the SW-W and the usual coastal drift towards the East, would have caused a transport of sediments towards the Punta Umbría breakwater. These processes would have been intensified by the torrential rains that increased the flow of the Piedras River, as well as by very high  $H_s$  (maximum for all existing records in 1996–2018). In addition, the spring tides and low pressures justified the annual maximums of sea level recorded between March 1st and 4th, 2018 (sea level up to 4.12 m). Therefore, the combined effect of low pressures, spring tides and wind in the direction of the beach would mean that the sea could have risen 2.3 m above the average level [42]. This increase, besides a highly erosive effect on the beach, could have affected the burial and mobilization of benthic organisms, accentuated by the large swell. The damage caused to the lighthouse located at the end of the Punta Umbría dock, on the afternoon of March 1st, 2018 [43] serves as an indicator of the force reached by the swell during the passage of storm Emma.

In addition, the presence of a curved dock at the eastern end of the Punta Umbría beach would have played an important role in the stranding, as suggested by the accumulation of organisms only at the eastern end of the El Portil-Punta Umbría stretch. This curved jetty was built in 1986, with the main objective of acting as a sediment trap to reverse the coastal regression that threatened some buildings near the high tide line. As a consequence, since the construction of the curved dock and other actions in the neighboring Ria de Huelva (mouth of the Tinto and Odiel rivers), the sedimentary dynamics have been altered. The waves are accumulating sediment on the western side of the curved dock, causing the accretion of the beach at a rate of 1.1 m/year [44].

Likewise, the SW-W winds, which are dominant in the area (22.5%) [44], would have favored the dock acting as a dead end for the organisms carried by the strong waves and the intensified coastal drift. In fact, the situation of continued low pressure did not end until March 7th, which would explain why the arrival of benthic organisms persisted for several days after the notable stranding of starfish documented by the local media on March 4th [45]. In sum, our results suggest that the extreme climatic conditions occurred during storm Emma provoked a combination of sediment burial and subsequent drag to the beach of benthic marine animals (most of them invertebrates), in accordance with [6].

The composition of stranded organisms here reported suggests that not all benthic fauna is equally sensitive to extreme stormy events. Following this reasoning, stranded animals, such as *Upogebia* spp., *Sipunculus nudus*, *Atelecyclus undecimdentatus* or *Lutraria lutraria* would have a lower resistance to burying and trawling during extreme stormy events than other crabs or molluscs, such as *Portunus latipes* and *Donax trunculus* that were not present (or were under-represented) in the mass stranding. The most abundant species present in the stranding (i.e., *Upogebia* spp.) excavate deep, complex galleries (e.g., up to 68 cm in *Upogebia deltaura*) [46], or remain deep-burrowed since early stages (e.g., *Pharus legumen* and *Lutraria lutraria* are buried at depths greater than 15 cm) [47] or have a limited resistance to re-burrow after sediment disturbance. For example, repeated exposure to the sediment surface would constitute a weak point for *L. lutraria*, due to its limited capacity to re-burrow after 48 h [40]. *Sipunculus nudus* colonizes sediments from the intertidal zone to depths of 160 m [48], and lies buried in the sand without building an elaborate gallery. It only forms a small funnel above the anterior part of the body that gives it access to water to breathe [49]. Occasionally, *S. nudus* can dig rapidly when the action of the waves pulls it out of the sand; however, the energy required by such muscular activities exceeds what it can generate with its aerobic metabolism, requiring activating an anaerobic metabolism [50]. Despite the ability of *S. nudus* to combine aerobic-anaerobic metabolisms, this species exhausts after 15 digging events in 45 min [50]. In contrast, the absence of *Donax trunculus* among the stranded organisms, a common bivalve of intertidal and shallow subtidal zones (between 0 and 6 m depth on the Atlantic coast), may be explained by its ability to fast and repeated burrowing (mean burrowing times = 14–65 s in fine and medium sands) [51]. This ability represents an adaptation to avoid the risk of surface transport and stranding on the swash zone, where highly frequent disturbance occurs [52]. In this sense, *D. trunculus* and *L. lutraria* show opposing strategies, adapted to very different environments, i.e., much more stable in the case of the long-living bivalve *L. lutraria* and

highly disturbed in the case of *D. trunculus* (that shows a shorter life cycle). This suggests that *L. lutraria* is much more vulnerable to extreme sediment transport events than *D. trunculus*. Simulations support this hypothesis and suggest that benthic organisms living at a water depth between  $-10$  m to  $-0.3$  m were buried under a layer of sediment of up to ca. 10 cm deposited during storm Emma. This burial preceded the transport of intertidal and subtidal benthic organisms to the dry beach, causing their stranding. The composition of the stranded organisms provides evidence of the outstanding magnitude of disturbance that affected the sea bed during storm Emma. The presence of the starfish *Astropecten* sp. is also rather surprising because these animals use to migrate offshore into deeper waters during the winter months probably to avoid strong onshore wave surges [53].

#### 4.3. Ecological consequences of the stranding

In relation to the possible effects of stranding on biodiversity, resilience and ecosystem services, the high density of mud shrimp (*Upogebia deltaura* and *Upogebia pusilla*) was alarming. *Upogebia pusilla* colonizes fine and muddy sands from the intertidal area to 6 m. *Upogebia* spp. dig deep galleries that ventilate through the action of their pleopods [46,54]. This way, the bioturbation activity of *Upogebia* spp. influences the biogeochemistry of marine sediments, increasing the area available for the exchange of solutes between the sediment and the water column, as well as the thickness of the oxygenated layer of the sediment. This activity, in turn, increases microbial processes, such as denitrification [55]. These decapods are considered the most abundant organisms of the sandy and maerl seafloors, with densities that can reach 100–200 indiv/m<sup>2</sup> [46,54,56], which would coincide with its relative abundance in the studied case of stranding. For this reason, *Upogebia* spp. offer an ecosystem service related to the release of a part of the anthropogenic nitrogen load in coastal waters, which in turn would have a beneficial effect on the quality of the habitat and its associated community [55]. Therefore, the mass mortality of gebiid decapods observed after storm Emma would result in a reduction in the degree of bioturbation and oxygenation of the sediment and the biogeochemical processes that occur at the water-sediment interface. Moreover, due to its high abundance in coastal sediments, the massive mortality of *Upogebia* spp. could cause cascade effects on other taxonomic groups, including predators of commercial interest [57–59]. The massive stranding of benthic ascidians could also lead to certain levels of reduction in the quality of the habitat. Although its role as filter feeders is not considered relevant in marine trophic networks unlike pelagic tunicates (e.g., salps), in situations of shallow or typically turbid waters, such as those existing in the study area, the massive loss of benthic ascidians may have a negative influence on the quality of water or on phytoplankton [60,61]. Likewise, the massive stranding of starfish may involve additional changes in community composition regarding their ecological role as high-level predators of intertidal and subtidal benthic communities, where they promote heterogeneity and diversity [62–64]. Particularly, *Astropecten* spp. (Fam. Astropectinidae) are voracious predators, feeding mainly on gastropods and bivalves.

The stranding also revealed that severe storm events involve the deposition of a large amount of macrodetritus (dark particles on the beach). This type of material usually accumulates in the marshes and the river basin. During the storm, which was accompanied by rains, this material was likely dragged by the river Piedras and other torrents to the beach [65]. Being of vegetable origin, it has positive buoyancy, which explains why it was deposited in the upper limit of the swash zone. Despite it may have a positive impact on terrestrial dune vegetation (providing an extra nitrogen input), the accumulation of such macrodetritus on the sediment surface involved a change of the habitat properties that may have affected benthic organisms (i.e., impeding the construction of galleries by gebiid decapods typical of fine sands and muddy sediments).

Regarding the duration of the effects of the mass mortality, the longevity data of the animals found suggests that it will take several years to recover the levels of abundance and biomass that the affected species presented before storm Emma. For example, the documented longevity for *Upogebia pusilla* and other members of the Gebiidea and Axiidea families is between 3 and 5 years [66]. In sum, the exceptional climatic and oceanographic events occurred during storm Emma (including the occurrence

of the maximum wave heights recorded in more than 20 years) and the variety of organisms affected, we suggest that the stranding here documented could be cataloged as ‘catastrophe’, according to [17]. An eventual increase in the frequency of this type of severe stormy events may involve worrying consequences in intertidal and subtidal communities, as well as the ecosystem services they provide. Our results are of interest both to marine biologists, but also to paleontologists as may help interpret similar mass mortality events in the fossil record [67].

**Supplementary Materials:** The executable file, cshore\_usace\_nosource-2015-11-09-09-45.tar, of the software CSHORE USACE version 2011, last edit 2015-11-09 and the input file, infile, with all the inputs used for the morphodynamic simulation of this study can be found here: <https://doi.org/10.5281/zenodo.3226991>.

**Author Contributions:** Methodology, J.G.-d.-L. and A.P.; software, A.P.; formal analysis, J.G.-d.-L., A.P. and J.A.C.; writing—original draft preparation, J.G.-d.-L., A.P. and D.M.; writing—review and editing, J.A.C. and D.M.; funding acquisition, A.P.

**Funding:** This research was partially funded by the UK Natural Environment Research Council (NE/M004996/1; BLUE-coast project).

**Conflicts of Interest:** The authors declare no conflict of interest. The funders had no role in the design of the study; in the collection, analyses, or interpretation of data; in the writing of the manuscript, or in the decision to publish the results.

## Appendix A

Additional information about CSHORE software can be found at <https://sites.google.com/site/cshorecode/>.

In the following appendix, the main software inputs are explained.

The CSHORE model requires an offshore (i.e., unaffected by refraction, shoaling and shadowing) wave data ( $H_{rms}$ ,  $T$  and  $\theta$ ), the Still Water Level (SWL) and Surge levels at the beginning and the end of the simulated period and the profile elevation. We have used the significant wave height,  $H_s$ , provided by the ‘Puertos del Estado’ buoy and the relationship  $H_s = 1.42 \times H_{rms}$  [27]. The wave angle was almost normal to the coast at the study site, and we have assumed normal incidence for the whole simulation. The SWL time series has been obtained from the Huelva 5 tide gauge. Because the recorded data at Huelva 5 already includes the astronomical and meteorological tide we have assumed storm surge = 0 m for the whole simulation.

Natural sediments are represented by the single diameter,  $d_{50} = 0.42$  [mm], specific gravity,  $s = 2.65$ , and fall velocity,  $w_f = 0.0592$  [m/s]. The fall velocity has been calculated using [68], and assuming water temperature of 15°C and water salinity 35 ppt.

We have used  $e_B = 0.005$  and  $e_f = 0.01$  as typical values in the computation of berm and dune erosion [19] where  $e_B$  and  $e_f$  = suspension efficiencies for the energy dissipation rates, due to wave breaking and bottom friction, respectively. The bottom friction,  $f_b$ , factor is of the order of 0.015 on sand beaches, but it should be calibrated using current longshore data because of the sensitivity of longshore currents to  $f_b$  [19]. The breaker ratio parameter  $\gamma$  is typically in the range of  $\gamma = 0.5$ – $1.0$ , but should be calibrated to obtain a good agreement with the measured cross shore variation of the standard deviation of the free surface elevation if such data are available. Because no data on free surface elevation were available, we have used the value of  $\gamma = 0.7$  for sandy beaches.

## References

1. Costa, P.R. Impact and effects of paralytic shellfish poisoning toxins derived from harmful algal blooms to marine fish. *Fish Fish.* **2016**, *17*, 226–248. [[CrossRef](#)]
2. Geraci, J.R.; Anderson, D.M.; Timperi, R.J.; St Aubin, D.J.; Early, G.A.; Prescott, J.H.; Mayo, C.A. Humpback whales (*Megaptera novaeangliae*) fatally poisoned by dinoflagellate toxin. *Can. J. Aquat. Sci.* **1989**, *46*, 1895–1898. [[CrossRef](#)]
3. Hewson, I.; Button, J.B.; Gudenkauf, B.M.; Miner, B.; Newton, A.L.; Gaydos, J.K.; Wynne, J.; Groves, C.L.; Hendler, G.; Murray, M.; et al. Dengue virus associated with sea-star wasting disease and mass mortality. *Proc. Natl. Acad. Sci. USA* **2014**, *111*, 17278–17283. [[CrossRef](#)]

4. Metzger, M.J.; Villalba, A.; Carballal, M.J.; Iglesias, D.; Sherry, J.; Reinisch, C.; Muttray, A.F.; Baldwin, S.A.; Goff, S.P. Widespread transmission of independent cancer lineages within multiple bivalve species. *Nature* **2016**, *534*, 705–709. [[CrossRef](#)] [[PubMed](#)]
5. McClintock, J.B.; McClintock, L.M.; Lawrence, J.M. Mass mortality of the sea stars *Luidia clathrata* and *Luidia alternata* on the Alabama coast, December 2013. *Gulf Mex. Sci.* **2013**, *31*, 7.
6. Brongersma-Sanders, M. Mass mortality in the sea. In *Treatise on Marine Ecology and Paleocology*; Hedgpeth, J.W., Ed.; Geological Society of America: Washington, DC, USA, 1957; Volume 67, pp. 941–1010.
7. Maynard, D.R.; Chiasson, Y. Storm related mortality of lobsters, *Homarus americanus*, on the northern shore of Prince Edward Island, Canada. *J. Shellfish Res.* **1988**, *7*, 169.
8. Ueno, S.; Kawano, M.; Mitsutani, A. Shell size of the paper nautilus *Argonauta argo* (Cephalopoda; Octopoda) stranded on a beach at the southernmost part of the Japan Sea in early winter. *J. Natl. Fish. Univ.* **1996**, *45*, 25–27.
9. Thorpe, J.; Spencer, E. A mass stranding of the asteroid *Asterias rubens* on the Isle of Man. *J. Mar. Biol. Assoc. UK* **2000**, *80*, 749–750. [[CrossRef](#)]
10. Sheehan, E.V.; Cousens, S.L. “Starballing”: A potential explanation for mass stranding. *Mar. Biodivers.* **2017**, *47*, 617–618. [[CrossRef](#)]
11. Penn, D.; Brockman, H.J. Age biased stranding and righting in male horseshoe crabs, *Limulus Polyphemus*. *Anim. Behav.* **1995**, *49*, 1531–1539. [[CrossRef](#)]
12. Dendy, A. Notes on a remarkable collection of marine animals lately found on the New Brighton Beach, near Christchurch, New Zealand. *Trans. N. Z. Inst.* **1897**, *30*, 320–325.
13. Patterson, A.H. *Notes of an East Coast Naturalist, a Series of Observations Made at Odd Times during a Period of Twenty-Five years in the Neighborhood of Great Yarmouth*; Methuen & Co: London, UK, 1904.
14. MacGinitie, G.E. Distribution and ecology of the marine invertebrates of Point Barrow, Alaska. *Smith. Misc. Coll.* **1955**, *128*, 1–201.
15. Ferber, I.; Lawrence, J.M. Distribution, substratum preference and burrowing behaviour of *Lovenia elongata* (Gray) (Echinoidea: Spatangoida) in the Gulf of Elat (“Aqaba”), Red Sea. *J. Exp. Mar. Biol. Ecol.* **1976**, *22*, 207–225. [[CrossRef](#)]
16. Gladfelter, W.B. General ecology of the cassiduloid urchin *Cassidulus cariberum*. *Mar. Biol.* **1978**, *47*, 149–160. [[CrossRef](#)]
17. Harper, J.L. *Population Biology of Plants*; Academic Press: London, UK, 1977.
18. Cai, W.; Borlace, S.; Lengaigne, M.; van Rensch, P.; Collins, M.; Vecchi, G.; Timmermann, A.; Santoso, A.; McPhaden, M.J.; Wu, L.; et al. Increasing frequency of extreme El Niño events due to greenhouse warming. *Nat. Clim. Chang.* **2014**, *4*, 111–116. [[CrossRef](#)]
19. Kobayashi, N. Coastal Sediment Transport Modeling for Engineering Applications. *J. Waterw. Port. Coast. Ocean Eng.* **2016**, *142*, 03116001. [[CrossRef](#)]
20. Rodríguez-Ramírez, A.; Morales, J.A.; Delgado, I.; Cantano, M. The impact of man on the morphodynamics of the Huelva coast (SW Spain). *J. Iber. Geol.* **2008**, *34*, 73–108.
21. CEDEX. *Estudio de La Dinámica Litoral, Defensa Y Propuesta de Mejoras En Las Playas Con Problemas: Estudio de Actuación del Tramo de Costa Comprendido Entre Las Desembocaduras de Los Ríos Guadiana Y Guadalquivir*; Secretaría de Estado de Medio Ambiente. Dirección General de Sostenibilidad de la Costa y del Mar: Madrid, España, 2013.
22. AEMET. 2018. Available online: <http://www.aemet.es/es/serviciosclimaticos/datosclimatologicos/valoresclimatologicos?l=4642E&k=and> (accessed on 26 March 2018).
23. CMAOT. *Programa de Gestión Sostenible del Medio Marino Andaluz: Informe Final de Resultados*; Consejería de Medio Ambiente y Ordenación del Territorio. Junta de Andalucía: Sevilla, Spain, 2017.
24. Ngoc-Ho, N. European and Mediterranean Thalassinidea (Crustacea, Decapoda). *Zoosystema* **2003**, *25*, 439–555.
25. Zariquiey-Álvarez, R. Crustáceos decápodos ibéricos. *Inv. Pesq.* **1968**, *32*, 510.
26. Gómez-Álvarez, G. *Guía de Las Conchas Marinas de Huelva*; Diputación de Huelva: Huelva, Spain, 2014; p. 214.
27. Thornton, E.B.; Guza, R. Transformation of wave height distribution. *J. Geophys. Res.-Oceans* **1983**, *88*, 5925–5938. [[CrossRef](#)]
28. Benavente, J.; Gracia, F.J.; Del Río, L.; Anfuso, G.; Rodríguez-Ramírez, A. Caracterización morfodinámica de las playas españolas del Golfo de Cádiz. *Bol. Geol. Min.* **2015**, *126*, 409–426.

29. Prieto, L.; Macías, D.; Peliz, A.; Ruiz, J. Portuguese Man-of-War (*Physalia physalis*) in the Mediterranean: A permanent invasion or a casual appearance? *Sci. Rep.* **2015**, *5*, 11545. [CrossRef] [PubMed]
30. Ocaña, O.; Alfonso-Carrillo, J.; Ballesteros, E. Massive proliferation of a dictyotalean species (Phaeophyceae, Ochrophyta) through the Strait of Gibraltar. *Rev. Acad. Canar. Cienc.* **2016**, *28*, 165–170.
31. Diario de Cádiz (March 4th). 2016. Available online: [http://www.diariodecadiz.es/elpuerto/Valdelagrana-plagada-conchas\\_0\\_1004899998.html](http://www.diariodecadiz.es/elpuerto/Valdelagrana-plagada-conchas_0_1004899998.html) (accessed on 15 July 2018).
32. Macías, D.; (Joint Research Centre, Ispra, Varese, Italy). Personal communication, 2018.
33. CNN, 6 March 2018. Available online: <https://edition.cnn.com/2018/03/06/europe/starfish-deaths-uk-beach-intl/index.html> (accessed on 9 April 2019).
34. Natural History Museum. 2018. Available online: <http://www.nhm.ac.uk/discover/news/2018/march/thousands-of-dead-starfish-wash-up-on-a-kent-beach.html> (accessed on 9 April 2019).
35. Ruppert, E.E.; Fox, R.S. *Seashore Animals of the Southeast: A Guide to Common Shallow-Water Invertebrates of the Southeastern Atlantic Coast*; Univercity South Carolina Press: Columbia, SC, USA, 1988; p. 429.
36. Holthuis, L.B. FAO species catalogue. Volume 13. Marine lobsters of the world. An annotated and illustrated catalogue of species of interest to fisheries known to date. *FAO Fish. Synop.* **1991**, *125*, 292.
37. Völkel, S. Sulfide tolerance and detoxification in *Arenicola marina* and *Sipunculus nudus*. *Am. Zool.* **1995**, *35*, 145–153. [CrossRef]
38. Fecher, R.; Grau, J.; Reichholf, J. *Fauna Y Flora de Las Costas*; Blume: Barcelona, Spain, 1992; p. 287.
39. Gaspar, M.B.; Santos, M.N.; Vasconcelos, P.; Monteiro, C.C. Shell morphometric relationships of the most common bivalve species (Mollusca: Bivalvia) of the Algarve coast (southern Portugal). *Hydrobiologia* **2002**, *477*, 73–80. [CrossRef]
40. Kerr, A.K. Aspects of the Biology of *Lutraria lutraria* (L.) (Bivalvia: Mactracea). Ph.D. Thesis, University of Glasgow, Glasgow, Scotland, 1981. Available online: <http://theses.gla.ac.uk/7448/> (accessed on 14 May 2019).
41. Lawrence, J.M. Mass mortality of echinoderms from abiotic factors. In *Echinoderm Studies 5*; Jangoux, M., Lawrence, J.M., Eds.; AA: Balkema, Rotterdam, 1996; pp. 103–137.
42. Muñoz, J.J.; Abarca, J.M. Effect of wind and atmospheric pressure variations on the mean sea level of salt marshes and estuaries. *Rev. Obras Públicas* **2009**, *3505*, 21–32.
43. ABCAndalucía, 2 March 2018. Available online: [http://sevilla.abc.es/andalucia/huelva/sevi-temporal-arranca-cuajo-faro-espigon-punta-umbria-201803022152\\_video.html](http://sevilla.abc.es/andalucia/huelva/sevi-temporal-arranca-cuajo-faro-espigon-punta-umbria-201803022152_video.html) (accessed on 14 May 2018).
44. Morales, J.A.; Cantano, M.; Rodríguez-Ramírez, A.; Martín Banda, R. Mapping Geomorphology and Active Processes on the Coast of Huelva (Southwestern Spain). *J. Coast. Res.* **2006**, *48*, 89–99.
45. ABCAndalucía, 5 marzo 2018. Available online: [http://sevilla.abc.es/andalucia/huelva/sevi-miles-estrellas-mar-aparecen-varadas-playa-huelva-causa-temporal-201803051116\\_video.html](http://sevilla.abc.es/andalucia/huelva/sevi-miles-estrellas-mar-aparecen-varadas-playa-huelva-causa-temporal-201803051116_video.html) (accessed on 14 May 2018).
46. Hall-Spencer, J.; Atkinson, R. *Upogebia deltaura* (Crustacea: Thalassinidea) in Clyde Sea maerl beds, Scotland. *J. Mar. Biol. Assoc. UK* **1999**, *79*, 871–880. [CrossRef]
47. Troncoso, J.S.; Urgorri, V. Distribución vertical de los moluscos en los sedimentos blandos de la Ría de Ares y Betanzos (Galicia, España). I. Metodología, caracterización de las estaciones y estructura faunística de los niveles. *Nova Acta Cient. Compostel. (Biol.)* **1992**, *3*, 145–160.
48. Saiz-Salinas, J.I. Los gusanos sipuncúlidos (Sipuncula) de los fondos litorales y circalitorales de las costas de la Península Ibérica, Islas Baleares, Canarias y mares adyacentes. *Monogr. Inst. Esp. Oceanogr.* **1986**, *1*, 1–84.
49. Hérubel, M.A. Recherches sur les sipunculides. *Mem. Soc. Zool. Fr.* **1907**, *20*, 107–418.
50. Pörtner, H.-O.; Kreutzer, U.; Siegmund, B.; Heisler, N.; Grieshaber, M.K. Metabolic adaptation of the intertidal worm *Sipunculus nudus* to functional and environmental hypoxia. *Mar. Biol.* **1984**, *79*, 237–247. [CrossRef]
51. De la Huz, R.; Lastra, M.; López, J. The influence of sediment grain size on burrowing, growth and metabolism of *Donax trunculus* L. (Bivalvia: Donacidae). *J. Sea Res.* **2002**, *47*, 85–95. [CrossRef]
52. Sassa, S.; Watabe, Y.; Yang, S.; Kuwae, T. Burrowing Criteria and Burrowing Mode Adjustment in Bivalves to Varying Geoenvironmental Conditions in Intertidal Flats and Beaches. *PLoS ONE* **2011**, *6*, e25041. [CrossRef] [PubMed]
53. Freeman, S.M.; Richardson, C.A.; Seed, R. Seasonal Abundance, Spatial Distribution, Spawning and Growth of *Astropecten irregularis* (Echinodermata: Asteroidea). *Estuar. Coast. Shelf Sci.* **2001**, *53*, 39–49. [CrossRef]
54. Tunberg, B. Studies on the population ecology of *Upogebia deltaura* (Leach) (Crustacea, Thalassinidea). *Estuar. Coast. Shelf Sci.* **1986**, *22*, 753–765. [CrossRef]

55. Howe, R.L.; Rees, A.P.; Widdicombe, S. The impact of two species of bioturbating shrimp (*Callinassa subterranea* and *Upogebia deltaura*) on sediment denitrification. *J. Mar. Biol. Assoc. UK* **2004**, *84*, 629–632. [[CrossRef](#)]
56. Dworschak, P.C. Feeding behavior of *Upogebia pusilla* and *Callinassa tyrrhena* (Crustacea, Decapoda, Thalassinidea). *Inv. Pesq.* **1987**, *51*, 421–429.
57. Posey, M.H. Predation on a burrowing shrimp: Distribution and community consequences. *J. Exp. Mar. Biol. Ecol.* **1986**, *103*, 143–161. [[CrossRef](#)]
58. Posey, M.H.; Dumbauld, B.R.; Armstrong, D.A. Effects of a burrowing mud shrimp, *Upogebia pugettensis* (Dana), on abundances of macro-infauna. *J. Exp. Mar. Biol. Ecol.* **1991**, *148*, 283–294. [[CrossRef](#)]
59. Hanekom, N.; Baird, D. Growth, production and consumption of the thalassinid prawn *Upogebia africana* (Ortmann) in the Swartkops Estuary. *S. Afr. J. Zool.* **1992**, *27*, 130–139.
60. Bone, Q.; Carré, C.; Chang, P. Tunicate feeding filters. *J. Mar. Biol. Assoc. UK* **2003**, *83*, 907–919. [[CrossRef](#)]
61. Petersen, J.K. Ascidian suspension feeding. *J. Exp. Mar. Biol. Ecol.* **2007**, *342*, 127–137. [[CrossRef](#)]
62. Christensen, A.M. Feeding biology of the sea star *Astropecten irregularis* Pennat. *Ophelia* **1970**, *8*, 1–134.
63. Jangoux, M.; Lawrence, J.M. *Echinoderm Nutrition*; Balkema, A.A., Ed.; CRE: Rotterdam, The Netherlands, 1982; p. 654.
64. Baeta, M.; Ramón, M. Feeding ecology of three species of *Astropecten* (Asteroidea) coexisting on shallow sandy bottoms of the northwestern Mediterranean Sea. *Mar. Biol.* **2013**, *160*, 2781–2795. [[CrossRef](#)]
65. Kotwicki, L.; Węśławski, J.M.; Raczyńska, A.; Kupiec, A. Deposition of large organic particles (macrodetritus) in a sandy beach system (Puck Bay, Baltic Sea). *Oceanologia* **2005**, *47*, 181–199.
66. Conides, A.J.; Nicolaidou, A.; Apostolopoulou, M.; Thessalou-Legaki, M. Growth, mortality and yield of the mudprawn *Upogebia pusilla* (Petagna, 1792) (Crustacea: Decapoda: Gebiidea) from western Greece. *Acta Adriat.* **2012**, *53*, 87–103.
67. Schäfer, W. *Ecology and Paleocology of marine Environments*; University of Chicago Press: Chicago, IL, USA, 1972.
68. Soulsby, R. *Dynamics of Marine Sands: A Manual for Practical Applications*; Thomas Telford: London, UK, 1997.



© 2019 by the authors. Licensee MDPI, Basel, Switzerland. This article is an open access article distributed under the terms and conditions of the Creative Commons Attribution (CC BY) license (<http://creativecommons.org/licenses/by/4.0/>).